J Comp Physiol A (1994) 175:749–759


ORIGINAL PAPER

E. Gaten

# Geometrical optics of a galatheid compound eye

Accepted: 20 May 1994

**Abstract** The eyes of galatheid squat lobsters (*Munida rugosa*) are shown to be of the reflecting superposition type. In the dark-adapted state corneal lenses focus light at the level of the rhabdoms and light from more than 1000 facets is redirected to the superposition focus by the reflecting surfaces of the crystalline cones. When the eye is light adapted, apposition optics are used. In this state paraxial light is focused by the corneal lens and the parabolic proximal end of the cone onto the distal end of a rhabdomeric lightguide. The latter transmits light across the clear zone to the rhabdom layer. In the dorsal part of the eye the individual ommatidia become progressively shorter until the cones and rhabdoms are no longer separated by a clear zone. Although formerly considered to be developing ommatidia, they are shown to be retained specifically for scanning the downwelling irradiance.

**Key words** Crustacea · Optics · Compound eye Lightguide · Superposition optics

**Abbreviations** *RI* refractive index
*SEM* scanning electron microscope

## Introduction

The eyes of galatheid squat lobsters have been well described at the light microscope level (Pike 1947; Kampa 1963, 1965; Bursey 1975; Fincham 1988) and the ultrastructure of the eye of the galatheid *Munida rugosa* has been described recently (Gaten 1990). These descriptions suggest that these eyes are of the reflecting superposition type (Land 1976; Vogt 1975), characterized by the presence of square facets over most of the cornea and the separation of the cone cell and retinula cell layers by a clear zone (Exner 1891; Land 1981b; Vogt 1977).

E. Gaten
Department of Zoology, University of Leicester, University Road, Leicester, LE1 7RH, UK

The optics of galatheid eyes have never been investigated, although they are generally assumed to use reflecting superposition optics as described for the eyes of shrimps, crayfish and lobsters (Land 1984a; Nilsson 1989). In a description of the eye of the galatheid *Pleuroncodes planipes*, Kampa (1963) questioned the existence of superposition image formation and suggested that light was transported to the rhabdoms via refractile lightguides.

The eyes of *M. rugosa* contain fusiform rhabdoms commonly found in superposition eyes, but they are modified by the possession of what are presumed to be distal rhabdomeric lightguides crossing the clear zone (Gaten 1990). These are formed by the eighth retinula cell alone in contrast to the similar lightguides seen in hermit crabs (Nilsson 1988) and in the moth *Ephestia* (Horridge 1971) where they are formed by all of the retinula cells.

In this paper, the formation of superposition images, the presence of lightguides across the clear zone and the presence of corneal lenses are demonstrated in the eye of *Munida rugosa*. The refractive indices of various components of the eye are measured and ray tracing techniques are used to estimate ray paths within the eye. The role of the dorsal region of the eye is also considered.

## Materials and methods

### Animals

*Munida rugosa* (Anomura: Galatheidae) is a squat lobster found around western Europe to a depth of over 1,250 m (Howard 1981). Specimens were obtained from Loch Torridon, Scotland, using creels at depths of 18 to 135 m. The creels were raised to the surface after the light level dropped below $6\times10^{17}$ photons $m^{-2}s^{-1}$ to avoid light-induced damage to the eyes.

Animals were kept in circulating seawater at 12°C (±2°) in tanks (0.6 m×1.1 m, 0.25 m deep) illuminated by green light ($\lambda$max=540 nm) giving a photon flux of $1.446\times10^{17}$ photons $m^{-2}s^{-1}$ at the bottom of the tank (similar to midday at 30 m depth in Loch Torridon: Gaten et al. 1990). The animals were kept on a 12 h light/12 h dark cycle (or a reverse 12 h dark/12 h light cycle). Animals were used either fully light- or dark-adapted, and fixation

**Table 1** Composition of decapod saline (made up in distilled water). Osmolarity=946 mOsmol, pH=7.5

| Molarity | Chemical | Volume |
|---|---|---|
| 0.54 *M* | sodium chloride | 890 ml |
| 0.54 *M* | potassium chloride | 14 ml |
| 0.36 *M* | calcium chloride | 38 ml |
| 0.36 *M* | magnesium chloride | 25 ml |
| 0.44 *M* | sodium sulphate | 42 ml |
| 0.01 *M* | HEPES buffer | 2.38 g |

or experimentation was carried out under the same light conditions as those under which they were routinely maintained.

To keep tissues alive a decapod saline solution was used (Table 1), based on that of Nilsson (1983a) with the inorganic composition adjusted to that of decapod blood (Robertson 1949).

### Eyeshine photography

To obtain in vivo photographs of eyeshine, animals were restrained in seawater. Changes occurring during light adaptation were recorded by photographing the eyeshine at intervals after switching on an adapting light (approximately $5\times10^{18}$ photons $m^{-2}s^{-1}$). The negatives were scanned using an LKB UltroScan XL Laser densitometer and the eyeshine brightness calculated (Shelton et al. 1992). The width of the eyeshine patch was measured from the densitometer scans.

### Superposition ray path demonstration

The formation of superposition images was investigated by photography, using a modification of the method of Land et al. (1979). Eyes were fixed for 0.5 to 1 h in 5% glutaraldehyde in decapod saline. A window was cut in the dorsal surface, removing a piece of cornea and underlying cones to expose the retina. The eye was attached to the base of a black perspex chamber with one side formed from a coverslip. The chamber was filled with seawater with fluorescein added to make the light path visible.

To obtain a narrow beam, light was passed through a lens and an iris diaphragm and focused onto a reducing telescope formed using two objective lenses. The light then passed through a second iris and was focused onto the eye with another lens. Both iris diaphragms were closed to produce a narrow beam (about 50 µm wide) at the cornea. The eye was traversed across the beam and photographed from above at different positions using a Zeiss photomacroscope and Kodak Tmax p3200 film.

### Eyecup preparation to demonstrate lightguides

Eyes were fixed in 5% glutaraldehyde in decapod saline for 2 to 4 h. A razor blade was used to make a preparation of the lateral part of the eye to include the cornea and cone layer, but not the retinula cell layer. This eyecup was photographed in a well slide using an inverted microscope, such that the preparation was observed from the clear zone and illuminated orthodromically (via the cornea). The same preparations were used to show the structure of the lightguides under the SEM. The eyecups were left in 0.2% buffered osmium tetroxide for 48 h to remove some of the cytoplasmic matrix (Tanaka and Naguro 1981). They were then dehydrated, critical point dried and observed using a Cambridge S100 SEM.

### Corneal lens focal length measurement

A cleaned cornea was mounted in a well slide filled with sea water and the space behind the cornea was filled with bovine serum albumen (Bryceson 1981). The microscope condenser was removed and a target (star 8 mm across) placed about 50 mm below the specimen (effectively at infinity for such a lens). The microscope was focused on the proximal face of the cornea and then refocused on the target. The calibrations on the fine focus of the microscope were used to estimate the focal length (back focal distance) of the corneal lens. These values were corrected for apparent depth (Galbraith 1955; Caveney and McIntyre 1981).

### Refractive index measurement by interference microscopy

Determination of the refractive indices of various optical elements was carried out using interference microscopy. The eyes were fixed in 5% glutaraldehyde in saline solution for 1 to 2 h to avoid cone damage during extraction. Fresh eyes could not be used due to the soft and unstable nature of the cones (Land 1976; Vogt 1977; Nilsson 1983b). The eyeshine or pseudopupil was observed during this period to ensure that no significant optical changes were occurring (D.-E. Nilsson, personal communication).

The eyes were transferred to fresh saline and the cornea, cones and rhabdoms dissociated. Isolated cones and rhabdoms were transferred to a slide and a coverslip was added, supported by other coverslips each 100 µm thick. Isolated elements were observed and photographed using a Zeiss Standard WL microscope and Sénarmont compensator together with an achromat ×40 objective lens and condenser. A 546 nm ($\lambda$) interference filter was inserted into the light path. The optical path difference ($\Delta\delta$) was determined using the formula:

$$\Delta\delta=(N+\phi)\cdot\lambda$$

where N=the number of interference fringes, ø is obtained from the reading on the analyzer (Varela and Wiitanen 1970). The measured optical path difference is a function of the specimen thickness and the difference in RI between the specimen ($n_0$) and the background medium ($n_1$), the latter being measured with an Abbé refractometer. The RI of the specimen was calculated as:

$$n_0=\Delta\delta/d+n_1$$

Where d=specimen thickness measured using an eyepiece graticule and stage micrometer.

## Results

### Eye structure

The eye of *M. rugosa* is approximately hemispherical and consists of a distal cone cell layer and proximal rhabdom layer, separated by an extensive clear zone (Fig. 1). When the eye is hemisected in the horizontal plane (Fig. 1B), most of the ommatidia are of similar length (c. 1000 µm). However, in the vertical plane (Fig. 1A) there is a clear gradient of ommatidial length, from a minimum dorsally to a maximum in ventro-lateral ommatidia. The most dorsal ommatidia are of the apposition type, with no tapetum or clear zone. There are around 12,000 ommatidia, each consisting of four cone cells (forming a crystalline cone), two corneagenous cells, two distal pigment cells and eight retinula cells (Gaten 1990). There is a reflective tapetum below the rhabdoms. The tops of the cone cells are separated by distal reflecting pigment cells which are presumed to reduce the light flux passing between the cones. Dark shielding pigments are present in the distal pigment cells and in the retinula

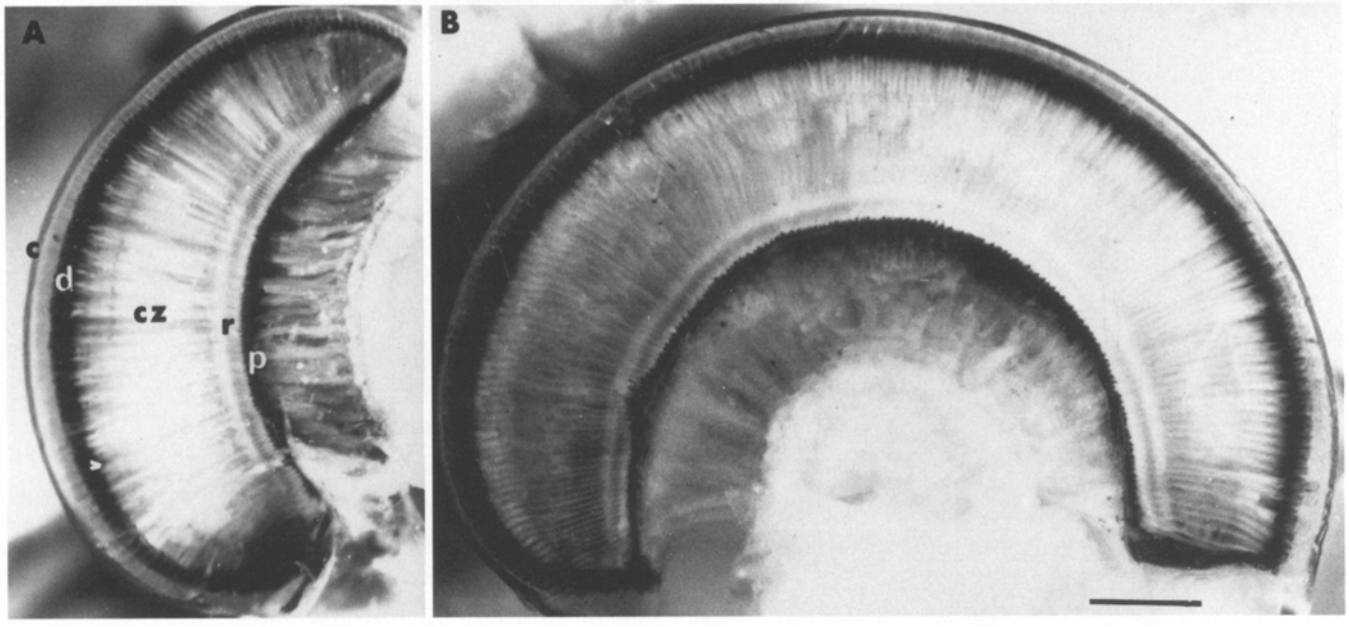


**Fig. 1** **A** Dorsoventral section through the eye to show the gradient of ommatidial length. The rhabdom layer (*r*) and the cone layer (*c*) get closer together dorsally (at the top of the picture) as the clear zone (*cz*) reduces considerably in width. In this dark-adapted eye, the proximal pigment (*p*) is located below the rhabdoms. **B** When the eye is sectioned horizontally it can be seen that the ommatidia are of a similar length throughout most of the section (anterior to the left of the picture). Scale bar: 500 μm

cells. In the latter they form two distinct populations. In the dark adapted state, the distal granules are located at the distal extremity of the retinula cells, between the sides of the crystalline cones and the proximal granules are found below the rhabdoms. During light adaptation the distal pigment moves proximally to surround the sides of the cone stalks, whilst the proximal retinula cell pigment moves distally to shield the rhabdom. The pigment in retinula cell 7 (R7) migrates across the clear zone in a thin column alongside the distal rhabdom (Gaten 1990) where it reduces the light flux within the light-guide.

## Eyeshine and pseudopupil observations

When a dark-adapted superposition eye is illuminated and viewed along the same axis, a circular patch of eyeshine can be seen because any light not absorbed is reflected back out of the eye by the tapetum (Fig. 2A). In many superposition eyes, the distal pigment provides what is effectively an iris (Stavenga 1979). During light adaptation proximal migration of the distal pigment reduces the diameter of the iris and hence the area of eyeshine, whilst the distal migration of retinula cell shielding pigment in front of the tapetum reduces the brightness of the eyeshine (Fig. 2B). Both the diameter and the intensity start to decrease after a short latent period (c. 10 min). The eyeshine is eventually replaced by a square black pseudopupil (Fig. 2C) showing that apposition optics are being used.

From the densitometric analysis of the photographs it can be seen that, following the latent period, the intensity of the eyeshine decreases logarithmically and the diameter of the eyeshine decreases linearly for the first hour of light adaptation. Both continue to decrease, though more slowly, throughout the observation period (Fig. 3).

In dark-adapted eyes brilliant eyeshine can be seen from all viewing angles except the most dorsal ones. The area of eyeshine is fairly constant over most of the eye and the diameter of the eyeshine spot can be used to estimate the *f*-number. The *f*-number (focal length/aperture), used to describe the light-gathering power of commercial lenses, can also be used as a measure of the sensitivity of eyes (Land 1981b; Nilsson 1990b). The value for the focal length is estimated as half the radius of the eye (Land 1981b), and the value for the aperture as the width of the eyeshine patch. The *f*-number for *M. rugosa* was 0.49 (s.d.=0.027) based on photographs of four eyes.

The interommatidial angle ($\Delta\varphi$) is important because the ability of the eye to resolve detail is ultimately dependent on the angular separation of the receptors, at least in those eyes having a 1:1 ratio of facet lenses to rhabdoms. The method used for determining $\Delta\varphi$ is to observe the movement of the pseudopupil as the eye is rotated (Kunze 1979; Stavenga 1979). The pseudopupil shows the location of ommatidia that are viewing the observer directly and appears as a dark spot that seems to follow the observer round as the eye is rotated. The mean value of $\Delta\varphi$ was 1.60 (s.d.=0.25), based on five eyes from three *M. rugosa*. Measurements taken from sections through the centre of the eye gave a $\Delta\varphi$ value of 1.58° (s.d.=0.22).

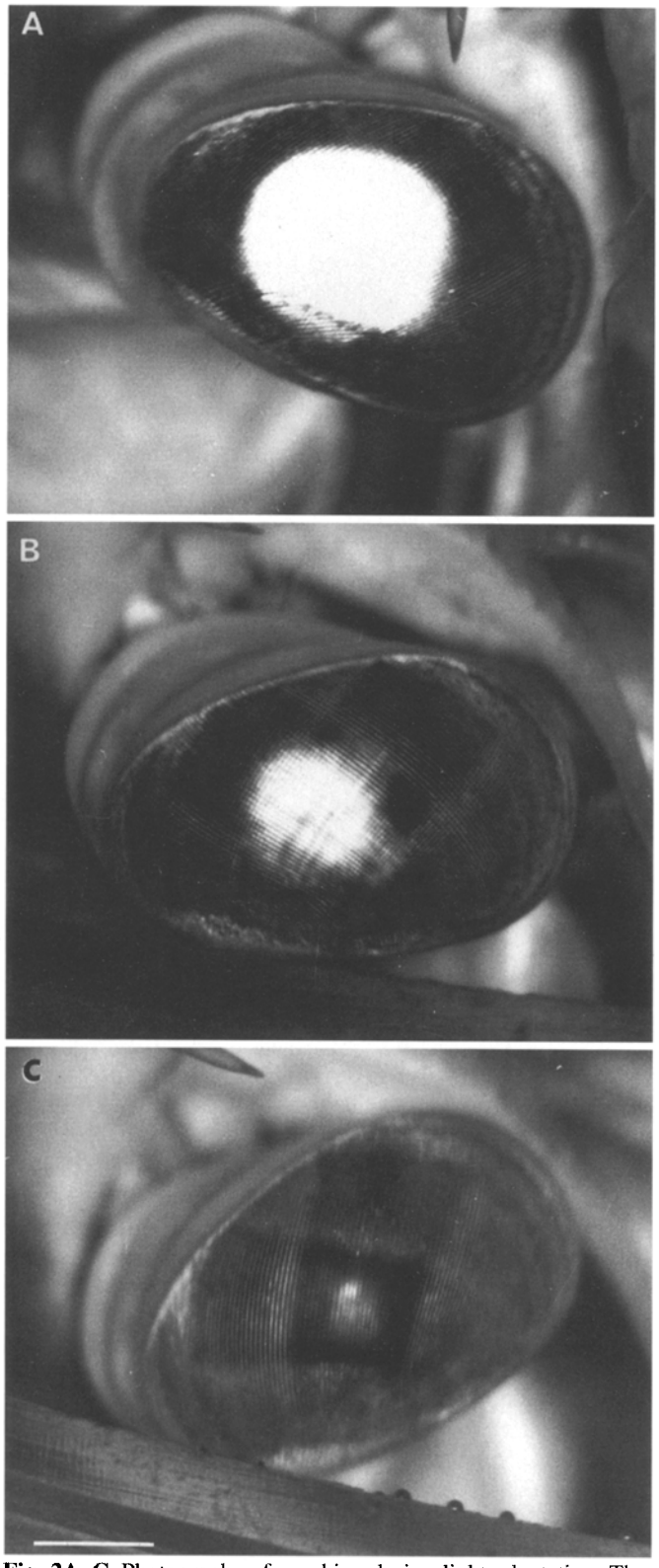


**Fig. 2A–C** Photographs of eyeshine during light adaptation. The brilliant eyeshine seen in the dark-adapted eye (**A**) is reduced in both extent and brightness after 30 min light adaptation (**B**). The fully light-adapted eye (**C**) shows a square black pseudopupil with the eyeshine reduced to a small central spot. Scale bar: 1000 μm

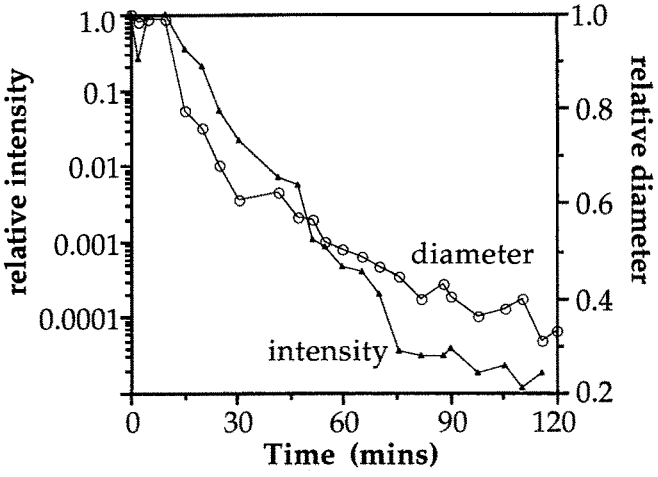


**Fig. 3** Relative change in the intensity (on a log scale) and the diameter of the eyeshine patch during light adaptation

## Superposition ray path demonstration

Although the formation of superposition images by clear zone eyes was disputed for many years, such ray paths have now been demonstrated in refracting superposition eyes (Horridge et al. 1982; Land et al. 1979), parabolic superposition eyes (Nilsson 1988) and reflecting superposition eyes (Vogt 1980).

When a narrow beam of light is shone onto an eye, the path of the light within the eye can be viewed through a hole cut in the cornea. When the light is traversed across the eye, the incident rays are redirected to a focus in the retinula cell layer. The ray path can be clearly seen although some scattering, thought to be due to fixation and preparation artefacts, occurs within the clear zone (Fig. 4). The angle of the incident ray, with respect to the ommatidial axis, is approximately equal to that of the reflected ray. When the centres of the rays are traced and superimposed on a drawing of the eye, it can be seen that they are brought to a focus in the retinula cell layer (Fig. 5).

## Demonstration of lightguides

When an eyecup is illuminated from the corneal surface and the cut ends of the distal rhabdomeres are viewed, it can be clearly seen that the latter act as light-guides (Fig. 6A). When the eyecups were observed with the SEM the square light-guide could be seen with retinula cell ribbons extending from each side (Fig. 6B). Considerable variation in the width of the light-guides was observed, from 2.0 to 6.5 μm (mean=4.06 μm, s.d.=0.98, $n$=18).

Throughout this paper it has been assumed that ray paths within the eye can be described purely by geometrical optics. This is not the case in eyes with very narrow rhabdoms because as the thickness of the receptor approaches the wavelength of light, they behave as waveguides. In these, light is propagated along the receptor as

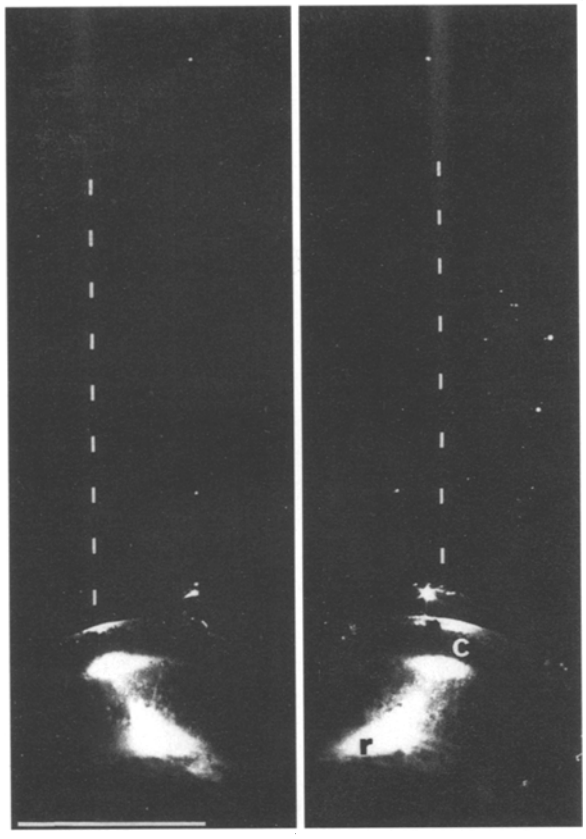


**Fig. 4** Two micrographs showing the redirection of light to form the superposition image. Narrow rays of light are redirected at the cone cell layer (*c*) and focused on the rhabdom layer (*r*). The path of the incident rays has been accentuated for clarity. Scale bar: 1000 μm

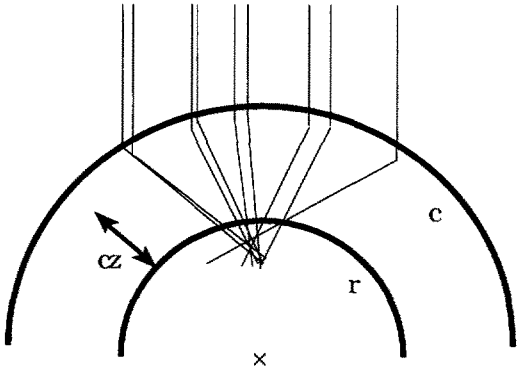


**Fig. 5** When the ray paths in micrographs such as Fig. 4 are traced onto the outline of the eye, it is apparent that parallel rays of light are directed to a focus within the rhabdom layer. Data from the lateral regions of two eyes (*c* cone layer; *cz* clear zone; *r* rhabdom layer; *x* centre of curvature of the cornea)

standing geometrical patterns known as waveguide modes. Most of the light is propagated along the waveguide, but outside of it (Land 1981b; Van Hateren 1989). The proportion of light outside the guide and the importance of waveguide effects is given by the waveguide parameter (V):

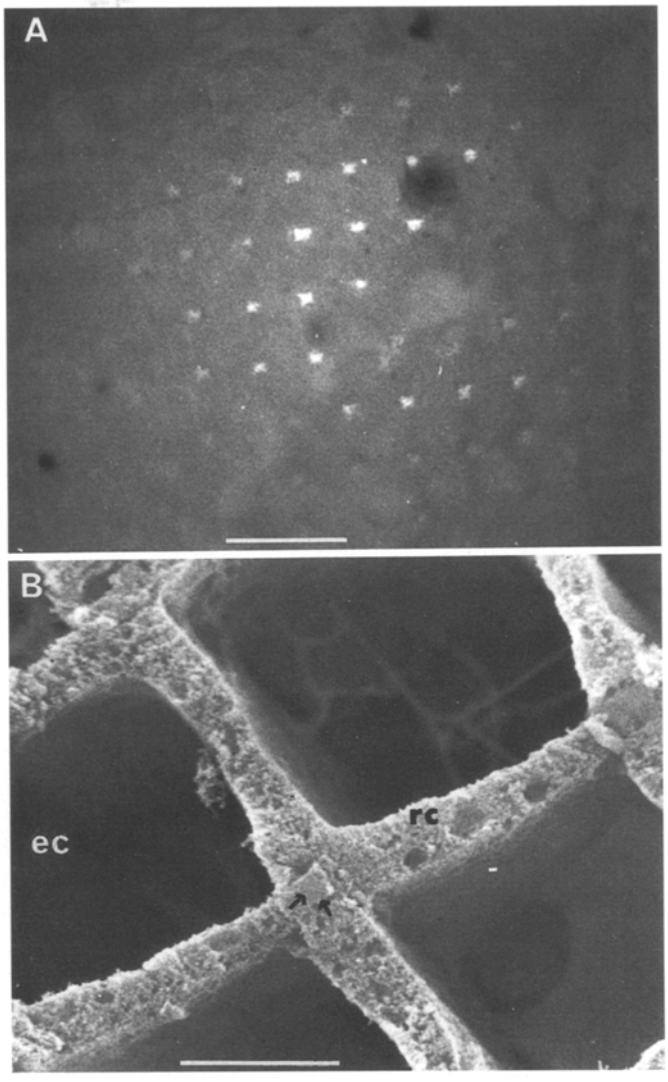


**Fig. 6** **A** The cut ends of the distal rhabdomeric lightguides appear as points of light in this eyecup preparation. Scale bar: 50 μm. **B** SEM of an eyecup preparation showing the square lightguides (*arrows*) separated by retinula cell ribbons (*rc*). Extracellular clear zone (*ec*) is enclosed by the lightguides at the corners and by the retinula cells along each side. Scale bar: 10 μm

$$V = \frac{\pi d}{\lambda} \cdot \sqrt{n_1^2 - n_2^2}$$

($\lambda$, wavelength of light; $d$, waveguide diameter; $n_1$ and $n_2$ RI of waveguide and cytoplasm) (Snyder 1975). When V=1, almost all light travels outside the waveguide, reducing to 10% when V=7 (Land 1981b). The thinnest receptor encountered in *M. rugosa* was the distal rhabdom with a diameter between 2.0 and 6.5 μm. As V=5.5 for the minimum recorded diameter, it appears that the distal rhabdom may function as a waveguide. However, a structure of this diameter should support four or more waveguide modes, so it will still behave according to geometrical optics (Van Hateren 1989).

**Table 2** Refractive index (mean and s.d. of *n* measurements) of the cornea, measured in the centre and at the edge of the facets, of mid-cone region, or rhabdoms and rhabdom threads

| Structure | RI mean | s.d. | *n* |
|---|---|---|---|
| Cornea (central) | 1.423 | 0.003 | 16 |
| Cornea (edge) | 1.417 | 0.003 | 16 |
| Cone cell cytoplasm | 1.365 | 0.007 | 14 |
| Mid-cone | 1.428 | 0.008 | 56 |
| Retinula cell cytoplasm | 1.346 | – | 2 |
| Rhabdom | 1.378 | 0.006 | 16 |
| Rhabdom thread | 1.394 | 0.021 | 5 |

## Corneal lenses

A good image is obtainable through the cornea of *M. rugosa* although the target remains in focus over a considerable range (±20% of the best focus). The focal lengths of 12 lenses from the centre of an unfixed cornea were measured with bovine serum albumen inside the cornea and seawater outside. The corrected mean back focal distance was 816 µm (s.d.=71.2).

Although the focal point cannot be determined accurately by this method, it is clear that pencils of light leaving each facet are focused deep within the eye and that the best focus would have occurred in the distal rhabdom layer.

## Refractive index measurements

### *Cornea*

Isolated and cleaned fragments of cornea from the centre of the eye were examined. The RI of the cornea varies across each facet, reaching a maximum in the centre of the facet (Table 2). In *M. rugosa* most of the refractive power must come from the internal lens structure, formed by the RI gradient, as the inner and outer faces of the corneal facet are only slightly curved. The refractive power of such facets is limited with the cornea in water, in contrast to the eyes of terrestrial insects where the curvature of the facet is sufficient to focus light onto the rhabdoms.

### *Crystalline cone cells*

The RI was measured at intervals down the middle of the crystalline cone and the proximal cone stalk (Table 2). The RI of the cone is constant over most of its length, decreasing sharply at the distal and proximal ends (Fig. 7). Interference micrographs of cone cross sections show that they are of constant RI with a narrow band of lower RI cytoplasm around the edge.

In the cone stalk, the RI decreases along a distal to proximal gradient as seen in other reflecting superposition eyes and approximately follows the function:

$$n_y = n_m\left[1+\left(\frac{\sin\delta}{y+\cos\delta-1}\right)^2\right]^{0.5}$$

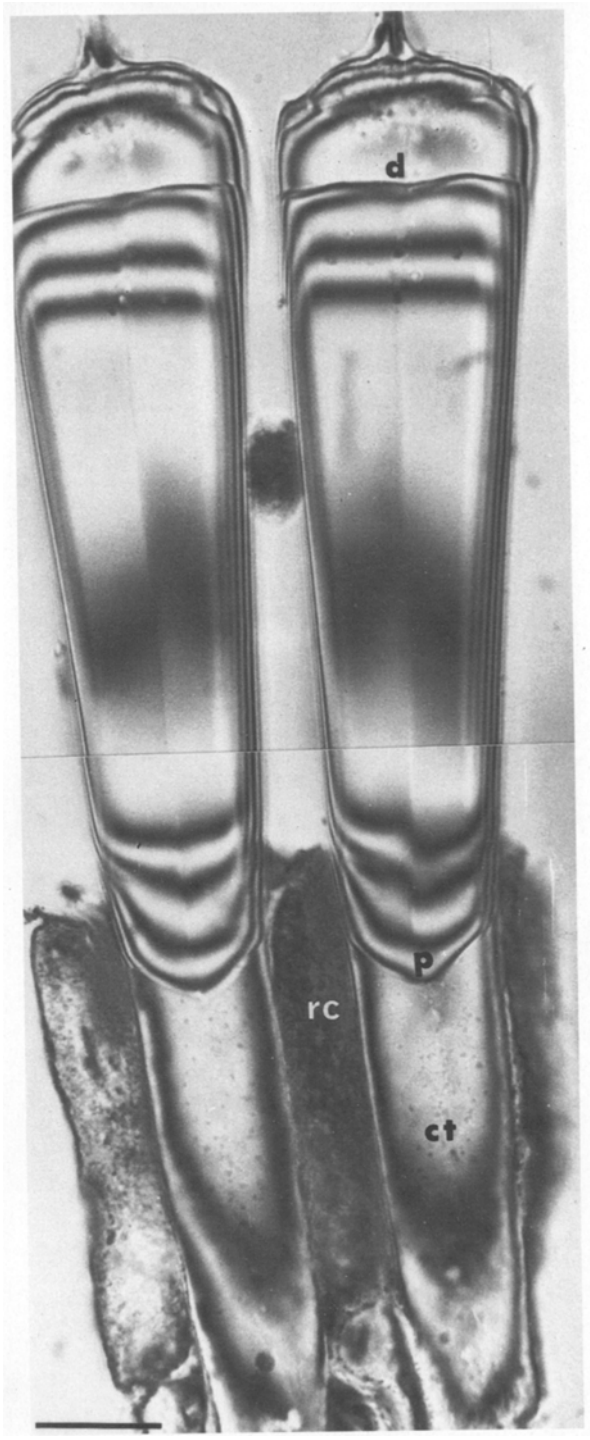


**Fig. 7** Interference micrograph of two isolated cones showing straight sides, constant internal RI and sharp fall in RI at the proximal (*p*) and distal (*d*) ends of the cone. At the proximal end of the cone and at the distal end of the stalk (*ct*), the curvature of the interference fringes shows that a radial gradient of RI is present. Retinula cells (*rc*) are present between the cone stalks. Scale bar: 20 µm

where y is the relative distance from the distal end of the cone, $n_y$ is the RI at y, $n_m$ is the RI of the cytoplasm and $\delta$ is the angle between the sides of the cone (Vogt 1977). The measured RI gradient of the crystalline cone cells

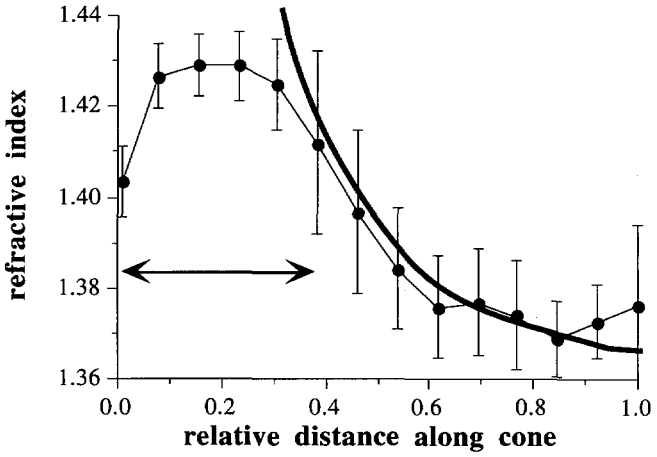


**Fig. 8** Change in RI with distance from the distal end of the cone (0) to the proximal end of the cone stalk (1.0) (mean of 12 cones±s.d.). The extent of the crystalline cone is shown by the *arrow*. The theoretical curve (*thick line*) is calculated after Vogt (1977), as described in the text, using a cone angle ($\delta$) of 7°

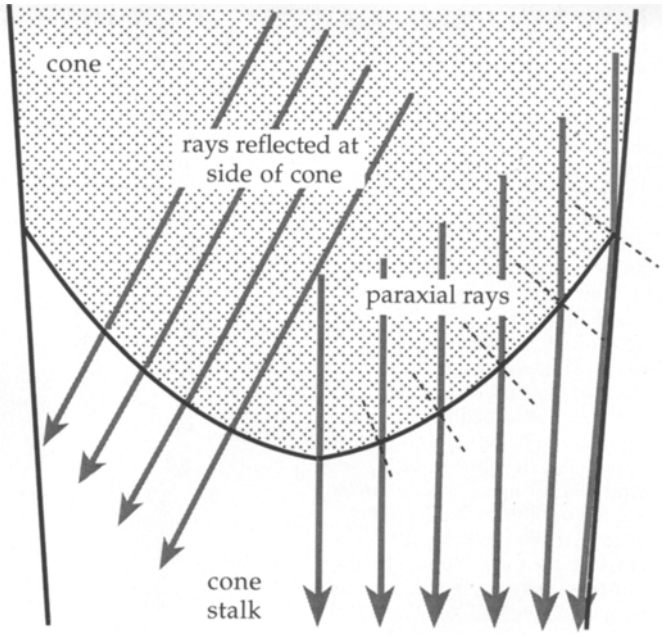


**Fig. 9** Proximal cone tip of *Munida rugosa* showing how the direction of light rays influences the way in which they are focused. Rays parallel to the ommatidial axis (right hand half of diagram) are focused onto the end of the lightguide by the parabolic cone tip. Rays that have been reflected at the cone wall (left hand half of the diagram) are more or less normal to the proximal boundary of the cone and are not focused to the same extent

and the theoretical curve agree well over the length of the cone stalk (Fig. 8).

In the cones, where the RI does not vary radially, the interference fringes run straight across (Fig. 7). However, at the proximal end of the cone and the distal part of the stalk the interference fringes are curved, indicating that the RI is highest in the centre and decreases radially (Fig. 7).

### *Rhabdoms*

The RI of the distal rhabdom threads was larger than that of the main rhabdoms (Table 2). However, the RI of the thread may be inaccurate as the retinula cell debris attached to the thread made it difficult to measure the width accurately using the interference microscope.

## Ray tracing

In *M. rugosa* the shape of the crystalline cone has a considerable effect on the ray path within the eye. The distal face of the cone is fairly flat and will have little effect on paraxial rays, although rays inclined to the ommatidial axis will be refracted. The proximal end of the cone has a characteristic parabolic profile. To illustrate this, three isolated, lightly-fixed cones were photographed, traced and the mean profile of the cone tip drawn (Fig. 9). When paraxial rays are incident on the proximal boundary of the cone, the central rays will pass through undeviated whereas the more peripheral rays are refracted by up to 1.6°. However, rays that have been reflected at the side of the cone will cross the ommatidial axis and leave the proximal cone more or less normally with a maximum refraction of around 0.5° (Fig. 9). The net result of this is that reflected rays remain focused in the region of the proximal rhabdom layer, whereas paraxial rays, already partially focused by the corneal lens, are refracted again at the proximal cone tip. Here, the combined action of the sharp change in RI at the cone/stalk boundary and the radial RI gradients in the proximal cone and in the distal stalk results in paraxial rays being brought to a focus on the distal tip of the rhabdomeric light-guide.

The most peripheral paraxial rays passing through the corneal lens are refracted by the combined lens system by between 3.5° and 4°. Thus in a cone stalk where the sides are around 3.5° to the ommatidial axis, all rays passing through the lens will be focused onto the end of the light guide. The parabolic shape of the cone lens ensures that a well-focused image is formed on the light guide, in contrast to a hemispherical lens which would suffer from spherical aberration.

In the light-adapted eye, most rays of light incident at up to 2° to the ommatidial axis are captured by the light guide (Fig. 10). Some rays are redirected onto the side of the stalk, which is lined by shielding pigment in the distal retinula cells (see Gaten 1990). This pigment will raise the RI outside of the stalk, causing these rays to leave the stalk and be absorbed. In the dark-adapted eye the screening pigment no longer lies alongside the cone stalk so these rays will be captured by total internal reflection and retained by the light guide. All light incident at 4° or more is absorbed by the shielding pigments in the light-adapted eye.

In the dark-adapted eye, all rays at more than 4° to the ommatidial axis that are not absorbed by the distal

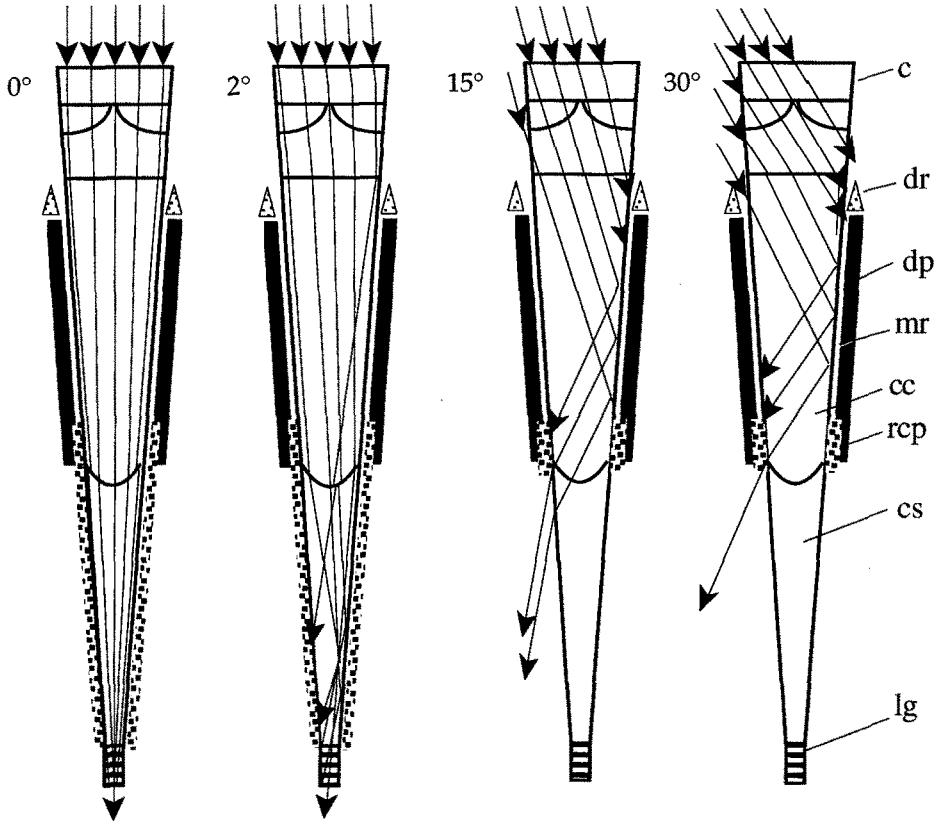


**Fig. 10** Diagram of the paths of axial rays (0°) and rays at 2° to the ommatidial axis through light-adapted cones. All of the rays at 0° are focused onto the distal end of the light guide. Of those rays incident at 2°, some reach the light guide whilst others are absorbed by the retinula cell shielding pigment that lines the tract. Above 4° all rays are absorbed in the light-adapted eye. The path of rays at 15° and 30° to the ommatidial axis is shown through dark-adapted cones. Most of the rays at 15° are absorbed by the cone pigments. The remaining rays pass out of the cone stalk, which is not lined by shielding pigment in the dark-adapted state. At 30° (the limit of rays entering the eyeshine patch) almost all rays are absorbed. (*c* cornea; *cc* crystalline cone; *cs* cone stalk; *dp* distal shielding pigment; *dr* distal reflecting pigment cell; *lg* lightguide; *mr* reflecting multilayer; *rcp* retinula cell shielding pigment)

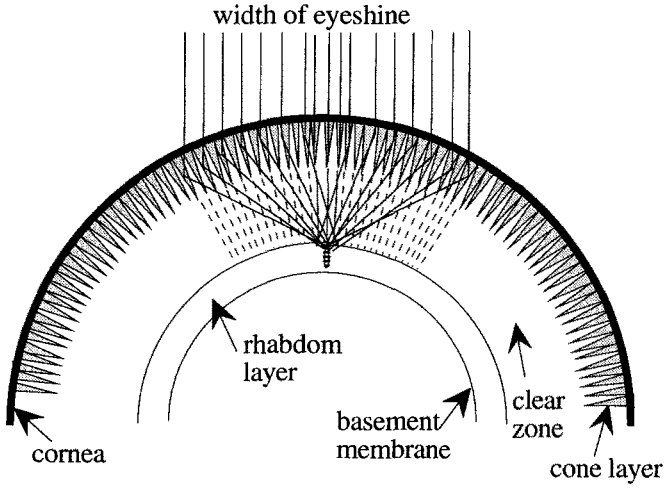


**Fig. 11** Ray tracing showing superposition image formation in a horizontal section through the dark-adapted eye of *M. rugosa* using a model eye based on Gaten (1990). Incident rays making an angle of up to 4° with the ommatidial axis cross the clear zone in the light guides. Those between 4 and 30° are focused in the middle of the rhabdom layer. Radii of curvature of the basement membrane ~1.2 mm, and of the cornea ~2.2 mm

screening pigments leave the cone stalk and cross the clear zone. The proportion of incident rays passing through the cone decreases with increasing angle of incidence. At 15° less than half of the rays cross the clear zone, whilst at 30° almost all are absorbed (Fig. 10).When the ray tracings for each cone are drawn onto the model eye (Fig. 11) it appears that in the dark-adapted eye incident rays of less than 4° to the ommatidial axis are light-guided, whereas those between 4 and 30° are focused in the middle of the rhabdom layer. Based on these assumptions, the resulting blur circle has a diameter of approximately 6 rhabdoms (~10°).

## Discussion

### Optics

The eye of *Munida rugosa*, with its square facets, clear zone, eyeshine and observed ray path, clearly uses reflecting superposition optics in the dark-adapted state. During light adaptation, eyeshine diameter is reduced as the superposition rays are intercepted by proximal movement of the distal shielding pigments (Gaten 1990). Eventually the eyeshine is replaced by a pseudopupil, indicating that apposition optics are in use (Stavenga 1979). The intensity of the eyeshine drops rapidly during light adaptation as the proximal shielding pigments cover the tapetum.

Eyecup preparations have been used to demonstrate light guides in refracting superposition eyes (Horridge et al. 1982) and in apposition eyes (Varela and Wiitanen 1970). They are used here to show that the distal rhabdoms function as light-guides in *M. rugosa*. Narrow parallel-sided rhabdoms have been subjected to extensive optical analysis (Exner 1891; Snyder 1977; Van Hateren

1989). The presence of such rhabdoms in decapods is limited to the brachyuran crabs (Arikawa et al. 1987), some hermit crabs (Nilsson 1989) and larval decapods (Fincham 1980; Nilsson 1983a). The elongated distal rhabdoms found in *M. rugosa* and those described in parabolic superposition eyes (Nilsson 1988) have parallel sides and are of a higher RI than the surrounding cells and should therefore retain light incident on the distal end of the rhabdom. These lightguides are of optical significance only when the eye is light adapted. In the dark-adapted eye only a few central ommatidia will use the lightguides whilst most of the light contributing to superposition image formation passes obliquely through the lightguides with little or no deviation.

The distal rhabdom acts as a lightguide because paraxial light is focused onto its distal end, initially by the action of the corneal lens, with the proximal end of the cone forming a second dioptric element. Weak corneal lenses have been demonstrated in the reflecting superposition eyes of several decapod species (eg. Bryceson 1981; Nilsson 1983b). In *M. rugosa* the corneal lenses focus light deep within the eye, with the back focal distance approximately equal to the distance between the cornea and the receptor layer. Following reflection at one side of the cone, all rays contributing to the superposition image will leave the proximal cone tip with little further refraction. However, paraxial rays will be focused onto the distal end of the lightguide by the parabolic cone tip and the radial RI gradients in the cone stalk.

An axial RI gradient is present in the cone stalk of *M. rugosa*, similar to that seen in other decapods (Vogt 1980; Nilsson 1983b). A high RI in the distal stalk ensures that rays passing through the cone without striking the sides are reflected at the edge of the stalk. However, after a single reflection the correct functioning of the eye requires that all rays leave the stalk when they next strike the edge of the stalk. To ensure that this happens, the RI decreases proximally. The function defined by Vogt (1977) relating the decrease in RI to distance down the cone agrees well with the experimental results obtained for *M. rugosa*. In the region of the cone/stalk junction, the RI required by the theoretical curve becomes unphysiologically high. Distal to this the cone can only contribute to the superposition image by using the reflecting multilayer (Land 1972) which lines the sides of the cones (Vogt 1977; Gaten 1990).

Fusiform rhabdoms (found only in superposition eyes) maximize the capture of light focused on the rhabdom from the wide superposition aperture (Warrant and McIntyre 1991). The distal taper and the relatively high internal RI of the rhabdom means that most of the light directed to the target rhabdom will be captured rather than pass through into adjacent rhabdoms where it would cause loss of resolution (Warrant and McIntyre 1991).

## Resolution and sensitivity

The rhabdoms seen in *M. rugosa* combine the light-gathering features of fusiform rhabdoms in the dark-adapted state with the light-guiding properties of thin distal rhabdoms when light adapted. A similar combination can be seen in hermit crabs and brachyuran crabs that use parabolic superposition optics (Nilsson 1988).

The light-gathering power of the eye may be assessed by the *f*-number (Land 1981b). Most superposition eyes have small *f*-numbers between 0.5 and 0.6 (Warrant and McIntyre 1991; Nilsson 1990a), with reflecting superposition eyes having the smallest, often less than 0.5. The eye of *M. rugosa* is well adapted to make use of the limited light available with an *f*-number of 0.49. The effective *f*-number will be greater as a smaller proportion of the light entering facets at higher angles of incidence will reach the retina compared to that entering central facets.

The resolving power of an eye is usually defined in terms of the interommatidial angle ($\Delta\varphi$), acuity ($1/\Delta\varphi$) or the highest spatial frequency of a grating that can just be resolved ($1/(2\Delta\varphi)$) (Land 1981b, 1984a, 1989). The value obtained for $\Delta\varphi$ in the eyes of *M. rugosa* (1.6°) suggests that they are capable of high resolution. The resolving power of superposition eyes is not necessarily lower than that of apposition eyes. The resolution of apposition and superposition eyes of diurnal insects can be similar (Land 1984b) and the same may be true of animals from dim environments (Nilsson 1989). However, the ability of the eye to resolve detail depends on the quality of the optics as well as the anatomical distribution of the receptors (Land 1989). The spatial resolution of *M. rugosa* has been determined electrophysiologically (Gaten and Shelton 1993). The acceptance angle of the eye (the angular width of the directional sensitivity function at half of the maximum height) varied from 12.5° in the dark-adapted state, to 6.6° when light adapted. The discrepancy between the interommatidial angle and the acceptance angle must lead to oversampling of the environment, especially by the dark-adapted eye. In the light-adapted state the lowest recorded acceptance angle was 3°, suggesting that the eye is capable of fairly high resolution.

## The dorsal apposition zone

The most dorsally-directed region of the eye always uses apposition optics, lacking both clear zone and tapetum. In other decapods this has been described as a proliferation zone where new ommatidia are added at each moult (eg Parker 1895; Shelton et al. 1981). However, I suggest that apposition optics are found here for functional, rather than developmental, reasons. The principal evidence for this is the presence of an "equator" around the horizontal midline of the eyes as reported from various insects (see Shaw and Stowe 1982), crayfish (Nässel 1976), crabs (Kunze 1968; Stowe 1977) and *M. rugosa* (Gaten 1990). Either side of this line, the arrangement of

retinula cells within each ommatidium is a mirror-image of those from the other side. If all new ommatidia were added to the dorsal rim of the eye the "equator" would move progressively towards the ventral edge: this has never been described. The retinula cells cannot reorientate themselves at the midline or migrate around the rim of the eye because these cells must project their axons topographically onto the lamina at all stages of development. If new ommatidia are added at the anterior margin of the eye, as in other decapods (Hafner et al. 1982; Douglas and Forward 1989), the dorsal and ventral halves of the eye will grow at the same rate.

The optics required to effectively exploit the dorsal light field are different from those necessary for viewing more complex backgrounds (Land 1981c, 1989). In mesopelagic crustaceans most of the eye is used for detecting point sources against a dim, uniform background. As image brightness is proportional to the pupil aperture for point sources (Kirschfeld 1974), the superposition eye with its large aperture and high sensitivity is well-adapted to this task. However, to detect small objects against the downwelling light, the relationship between the acceptance angle of a receptor and the angle subtended by the object becomes important. In the absence of any object overhead, the dorsal ommatidia will be maximally stimulated by the downwelling light. Any object entering the field of view will cause the greatest decrement in the signal if it subtends an angle equal to the acceptance angle of the ommatidium, causing the signal to fall from a maximum (downwelling light) to a minimum (silhouette). If superposition optics were in use, a significant decrement in the signal would only occur if the object were very large or very close. Although a small acceptance angle is desirable for detecting silhouettes, this would reduce sensitivity by limiting the total number of photons available to the receptor (Land 1981b). However, according to Land (1981c, 1989) a large relative difference in photon numbers (small acceptance angle) is more important than large absolute numbers of photons (large acceptance angle). It is concluded from this that a dorsal apposition zone is the most efficient arrangement for exploiting the downwelling light.

Eye development in juvenile shrimps (Fincham 1984; Gaten and Herring, unpubl.) involves the gradual transition from apposition to superposition optics. In the early stages the eye uses apposition optics. The proportion of the eye using superposition optics increases at each larval moult until, in the adult eye, it covers all but the most dorsal regions. The ommatidia of the dorsal zone should therefore be considered as retained apposition ommatidia, rather than precursors of superposition ommatidia.

## Phylogeny

The version of the reflecting superposition eye described here differs from that seen in shrimps and crayfish (Vogt 1975; Land 1976) by the possession of a light guide. The development of such an eye from the larval apposition eye presents no problem. The formation of a clear zone, allowing the use of superposition optics, involves the elongation of the distal rhabdom (rather than the cone stalk, as in other reflecting superposition eyes). All intermediate stages, between eyes with lightguides and short cone stalks and those with cone stalks extending across the clear zone, should be functional.

Two alternative hypotheses covering the evolution of the galatheid type of eye are possible. The reflecting superposition eye found in other decapods may have been modified by the progressive change in relative lengths of the distal rhabdom and the cone stalk. Alternatively, reflecting superposition optics may have evolved independently in the galatheids. It has been suggested that the possession of reflecting superposition eyes may be a phylogenetic character, linking the galatheids and the long-bodied decapods (Fincham 1980; Land 1981a). It is probable that refracting superposition optics have evolved separately in the euphausiids and mysids (Land et al. 1979), caridean shrimps, hermit crabs (Nilsson 1990a) and in several insect orders (see Land 1981b). It may be, in the light of the widespread occurrence of refracting superposition eyes, that the evolution of superposition optics is not such a rare event and that the galatheid eye is related only functionally to that of other decapods.

**Acknowledgements** I thank Mr C.J. Chapman, Scottish Office Agriculture and Fisheries Division, for supplying the animals and Dr P.M.J. Shelton for his invaluable comments and discussions. This work was supported in part by NERC grant number GR3/5564.

## References

Arikawa K, Kawamata K, Suzuki T, Eguchi E (1987) Daily changes of structure function and rhodopsin content in the compound eye of the crab *Hemigrapsus sanguineus*. J Comp Physiol A 161: 161–174

Bryceson KP (1981) Focusing of light by corneal lenses in a reflecting superposition eye. J Exp Biol 90: 347–350

Bursey CR (1975) The microanatomy of the compound eye of *Munida irrasa* (Decapoda: Galatheidae) Cell Tissue Res 160: 505–514

Caveney S, McIntyre P (1981) Design of graded-index lenses in the superposition eyes of scarab beetles. Phil Trans R Soc Lond B 294: 589–632

Douglass JK, Forward RB (1989) The ontogeny of facultative superposition optics in a shrimp eye: hatching through metamorphosis. Cell Tissue Res 258: 289–300

Exner S (1891) Die Physiologie der facettirten Augen von Krebsen und Insecten. Franz Deuticke, Leipzig-Wien

Fincham AA (1980) Eyes and classification of malacostracan crustaceans. Nature 287: 729–731

Fincham AA (1984) Ontogeny and optics of the eyes of the common prawn *Palaemon serratus* (Pennant 1777). Zool J Linn Soc 81: 89–113

Fincham AA (1988) Ontogeny of anomuran eyes. Symp Zool Soc 59: 123–155

Galbraith W (1955) The optical measurement of depth. Q J Microsc Sci 96: 285–288

Gaten E (1990) The ultrastructure of the compound eye of *Munida rugosa* (Crustacea: Anomura) and pigment migration during light and dark adaptation. J Morphol 205: 243–253

Gaten E, Shelton PMJ (1993) Spatial resolution in benthic decapods, determined by electrophysiological measurement of acceptance angle. J Physiol (Lond) 467: 371P
Gaten E, Shelton PMJ, Chapman CJ, Shanks AM (1990) Depth-related variation in structure and functioning of the compound eyes of the Norway lobster *Nephrops norvegicus*. J Mar Biol Assoc 70: 343–355
Hafner GS, Tokarski T , Hammond-Soltis G (1982) Development of the crayfish retina: A light and electron microscopic study. J Morphol 173: 101–118
Horridge GA (1971) The retina of *Ephestia* (Lepidoptera). Proc R Soc Lond B 171: 445–463
Horridge GA, Marçelja L, Jahnke R (1982) Light guides in the dorsal eye of the male mayfly. Proc R Soc Lond B 216: 25–51
Howard FG (1981) Squat lobsters. Scottish Fisheries Bulletin 46: 13–16
Kampa EM (1963) The structure of the eye of a galatheid crustacean *Pleuroncodes planipes*. Crustaceana 6: 69–80
Kampa EM (1965) The euphausiid eye – a re-evaluation. Vision Res 5: 475–481
Kirschfeld K (1974) The absolute sensitivity of lens and compound eyes. Z Naturforsch 29c: 592–596
Kunze P (1968) Die Orientierung der Retinulazellen im Auge von *Ocypode*. Z Zellforsch Mikrosk Anat 90: 454–462
Kunze P (1979) Apposition and superposition eyes. In: Autrum H (ed) Vision in invertebrates (Handbook of Sensory Physiology, vol VII/6A) Springer, Berlin Heidelberg New York, pp 441–502
Land MF (1972) The physics and biology of animal reflectors. Progr Biophys Molec Biol 24: 75–106
Land MF (1976) Superposition images are formed by reflection in the eyes of some oceanic decapod Crustacea. Nature 263: 764–765
Land MF (1981a) Optical mechanisms in the higher Crustacea with a comment on their evolutionary origins. In: Laverack MS, Cosens DJ (eds) Sense organs. Blackie, London Glasgow, pp 31–48
Land MF (1981b) Optics and vision in invertebrates. In: Autrum H (ed) Vision in invertebrates (Handbook of Sensory Physiology, vol VII/6B) Springer,Berlin Heidelberg New York, pp 471–492
Land MF (1981c) Optics of the eyes of *Phronima* and other deep-sea amphipods. J Comp Physiol 145: 209–226
Land MF (1984a) Crustacea. In: Ali MA (ed) Photoreception and vision in invertebrates. Plenum Press, New York, pp 401–438
Land MF (1984b) The resolving power of diurnal superposition eyes measured with an ophthalmoscope. J Comp Physiol A 154: 515–533
Land MF (1989) The eyes of hyperiid amphipods: relations of optical structure to depth. J Comp Physiol A 164: 751–762
Land MF, Burton FA, Meyer-Rochow VB (1979) The optical geometry of euphausiid eyes. J Comp Physiol 130: 49–62
Nässel DR (1976) The retina and retinal projection on the lamina ganglionaris of the crayfish *Pacifastacus leniusculus* Dana. J Comp Neurol 167: 341–360
Nilsson D-E (1983a) Evolutionary links between apposition and superposition optics in crustacean eyes. Nature 302: 818–821
Nilsson D-E (1983b) Refractive index gradients subserve optical isolation in a light-adapted reflecting superposition eye. J Exp Zool 225: 161–165
Nilsson D-E (1988) A new type of imaging optics in compound eyes. Nature 332: 76–78
Nilsson D-E (1989) Optics and evolution of the compound eye. In: Hardie RH, Stavenga DG (eds) Facets of vision. Springer, Berlin, pp 30–73
Nilsson D-E (1990a) Three unexpected cases of refracting superposition eyes in crustaceans. J Comp Physiol A 167: 71–78
Nilsson D-H (1990b) From cornea to retinal image in invertebrate eyes. Trends Neurosci 13: 55–63
Parker GH (1895) The retina and optic ganglia in decapods especially in *Astacus*. Mitt Zool Stat Neapel 12: 56–63
Pike RB (1947) Galathea. Liverpool Mar Biol Comm Mem 34: 1–178
Robertson JD (1949) Ionic regulation in some marine invertebrates. J Exp Biol 26: 182–200
Shaw SR, Stowe S (1982) Photoreception. In: Atwood HL, Sandeman DC (eds) The biology of Crustacea. Academic Press, New York, pp 291–367
Shelton PMJ, Shelton RGJ, Richards PR (1981) Eye development in relation to moult stage in the European lobster *Homarus gammarus* (L.) J Cons Int Explor Mer 39: 239–243
Shelton PMJ, Gaten E, Herring PJ (1992) Adaptations of tapeta in the eyes of mesopelagic decapod shrimps to match the oceanic irradiance distribution. J Mar Biol Assoc 72: 77–88
Snyder AW (1975) Photoreceptor optics - theoretical principles. In: Snyder AW, Menzel R (eds) Photoreceptor optics. Springer,Berlin, pp 38–55
Snyder AW (1977) Acuity of compound eyes. Physical limitations and design. J Comp Physiol 116: 161–182
Stavenga DG (1979) Pseudopupils of compound eyes. In: Autrum H (ed) Vision in invertebrates (Handbook of Sensory Physiology, vol VII/6A) Springer,Berlin Heidelberg New York, pp 357–439
Stowe S (1977) The retina lamina projection in the crab *Leptograpsus variegatus*. Cell Tissue Res 185: 515–525
Tanaka K, Naguro T (1981) High resolution scanning electron microscopy of cell organelles by a new specimen preparation method. Biomed Res 2: 63–70
Van Hateren JH (1989) Photoreceptor optics theory and practice. In: Hardie RH, Stavenga DG (eds) Facets of vision. Springer, Berlin, pp 74-89
Varela FG, Wiitanen W (1970) The optics of the compound eye of the honeybee (*Apis mellifera*). J Gen Physiol 55: 336–358
Vogt K (1975) Optik des Flusskrebsauges. Z Naturforsch 30c: 691
Vogt K (1977) Ray path and reflection mechanisms in crayfish eyes. Z Naturforsch 32: 466–468
Vogt K (1980) Die Spiegeloptik des Flusskrebsauges. J Comp Physiol 135: 1–19
Warrant EJ, McIntyre PD (1991) Strategies for retinal design in arthropod eyes of low F-number. J Comp Physiol A 168: 499–512